Chemically Amplified Molecular Glass Photoresist Regulated by 2-Aminoanthracene Additive for Electron Beam Lithography and Extreme Ultraviolet Lithography

Siliang Zhang,[§] Long Chen,[§] Jiaxing Gao, Xuewen Cui, Xue Cong, Xudong Guo,* Rui Hu, Shuangqing Wang,* Jinping Chen, Yi Li, and Guoqiang Yang*

ACCESS | Metrics & More | Article Recommendations | SI Supporting Information

ABSTRACT: 2-Aminoanthracene was used as a nucleophilic additive in a molecular glass photoresist, bisphenol A derivative (BPA-6-epoxy), to improve advanced lithography performance. The effect of 2-amino-anthracene on BPA-6-epoxy was studied by electron beam lithography (EBL) and extreme ultraviolet lithography (EUVL). The result indicates that the additive can optimize the pattern outline by regulating epoxy cross-linking reaction, avoiding photoresist footing effectively in EBL. The EUVL result demonstrates that 2-aminoanthracene can significantly reduce line width roughness (LWR) for HP (Half-Pitch) 25 nm (from 4.9 to 3.8 nm) and HP 22 nm (from 6.9 to 3.0 nm). The power spectrum density (PSD) curve further confirms the reduction of roughness at medium and high frequency for HP 25 nm and the whole range of frequency for HP 22 nm, respectively. The study offers useful guidelines to improve the roughness of a chemically amplified molecular glass photoresist with epoxy groups for electron beam lithography and extreme ultraviolet lithography.
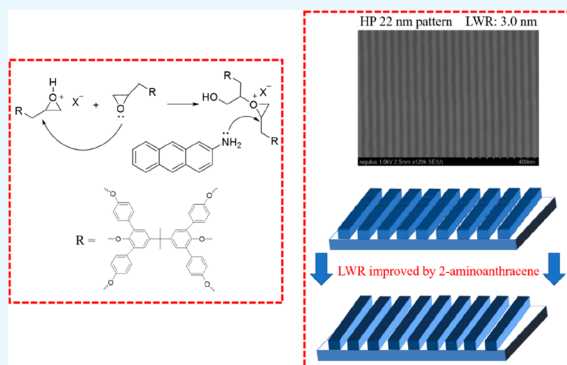
INTRODUCTION

With the continuous development of integrated circuits, lithography fabrication requires more advanced techniques to improve resolution.[1,2] Photoresist is one of the most critical materials in the lithography process, as a barrier layer, photoresist pattern is used to achieve selective etching and ion implantation, which play a decisive role in high-resolution lithography.[3] Since the development of 248 nm lithography, chemically amplified photoresists were introduced to improve the quantum yield. Chemical amplification photoresists mainly include polymer resin, photo acid generators (PAGs), solvent and other additives.[4] PAG is a photosensitive compound; in the post exposure baking (PEB) process, it will stimulate the reaction of the acid sensitive group on the main chain of the resin and generate new acid components. To improve lithography performance, the development of more advanced photoresist materials is significant.[5−10] Lawson's team designed molecules with epoxy structure and used them for negative-tone photoresist.[11−14] After exposure, PAGs generate photo-acid and catalyze the self-cross-linking reaction of the epoxy compounds, finally forming a dense network which drives the solubility switch. In addition, the huge cross-linked network can effectively improve the mechanical properties of the photoresist.

Compared with positive-tone photoresists, the active site of epoxy photoresists after exposure is the onium ion that reacts with the acid proton. Lawson et al. compared the DUV contrast curves of different trioctylamine (TOA, a common acid diffusion inhibitor) contents.[15,16] It is found that the content of trioctylamine in the system will not have a significant impact on the lithography performance. Combined with the mechanism of the cross-linking reaction, Lawson's team proposed to introduce nucleophiles to regulate the cross-linking reaction of epoxy molecules. Some common nucleophiles include molecules containing phosphorus and oxygen elements, which have been proven to significantly optimize contrast and achieve smaller half-pitch lithography pattern, and the groups formed by the above atoms connected with active protons can also play a role in regulating epoxy cross-linking reaction.[15] However, nucleophiles containing nitrogen are rarely reported to be used for high-resolution lithography. Manouras et al. studied the application of 2-aminoanthracene as an acid diffusion inhibitor (base quencher) in polymer chemically amplified backbone scission
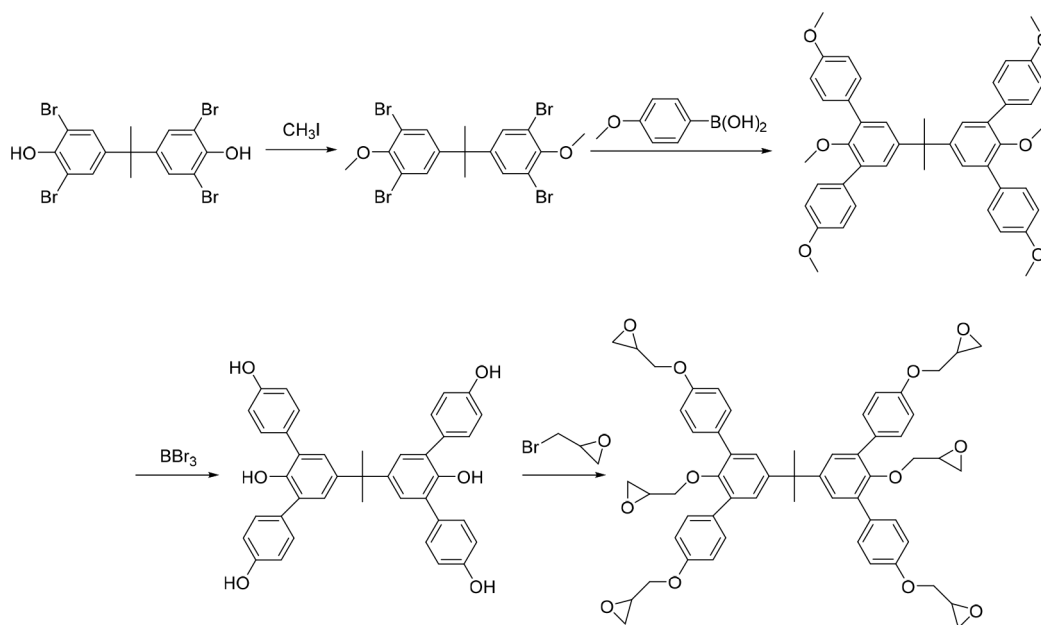
Scheme 1. Synthesis Route of BPA-6-Epoxy

photoresists, which can obtain 44 nm line/space (L/S) pattern in EUV lithography, and the line width roughness (LWR) was only 2.5 nm.[17]

The sensitivity of the photoresist is a very important parameter that determines the cost of semiconductor device manufacturing. Because the photoresist absorbs the incident light, the optical density is higher at the surface of the photoresist during the exposure process, resulting in lower energy at the bottom of the photoresist, which greatly limits the further improvement of resolution. For chemically amplified photoresist, acid-sensitive groups react with photo-acids and PAGs generate acid simultaneously, greatly improving the quantum yield of 248/193 nm and EUV chemically amplified photoresists.[18−20] However, it is difficult to effectively control the acid diffusion in the PEB process. For small pitches (critical dimension usually less than 40 nm), insufficient acid diffusion can lead to large LWR.[21−23] Therefore, analyzing the reasons for the LWR is one of the crucial problems that have to be solved for chemically amplified photoresists.

A molecular glass photoresist, bisphenol A derivative (BPA-6-epoxy), was designed and synthesized in our research group.[24,25] It can be used as a negative photoresist for EUVL and EBL with good monodispersity, exact molecular mass, and structure. After photoresist formulation and process optimization, dense lines with 44 nm pitch were achieved, but the LWR needs to be further improved. As the feature size gets smaller, the line roughness starts to have a non-negligible impact on the pattern size; it is necessary to find other ways to reduce the roughness of the patterns in anticipation of new molecular glass photoresists with higher resolution. In this paper, 2-aminoanthracene was used as a nucleophilic additive to regulate the epoxy cross-linking reaction and obtained good lithography results. The introduction of 2-aminoanthracene can also optimize the cross-section of the EBL pattern and significantly reduce the LWR of HP (Half-Pitch) 25 and 22 nm pattern in EUVL. The results may provide a useful choice for the practical application of the molecular glass photoresist.

EXPERIMENTAL SECTION

Materials. All chemical reagents are commercially available and can be used without additional treatment.

Synthesis of Molecular Glass BPA-6-Epoxy. BPA-6-epoxy was synthesized by our research group before.[24] The synthesized BPA-6-epoxy was evaluated by ^{1}H and ^{13}C NMR spectroscopy (Figures S1−S2).

Photolithography. BPA-6-epoxy (90 mg), triarylsulfonium hexafluoroantimonate salt (PAG, 9 mg), and 2-aminoanthracene (0.9 mg) were dissolved in 3 mL of propylene glycol methyl ether acetate (PGMEA) with 20 min ultrasonic treatment. The solution was filtered through a 0.2 μm polytetrafluoroethylene membrane filter twice and spin coated onto a silicon wafer with 2800 rpm/s for 90 s. Then it was baked at 80 °C for 180 s to remove PGMEA. The exposed samples were baked at 100 °C for 120 s, developed with 4-methyl-2-pentanone (MIBK) for 1 min, and rinsed with 2-propanol (IPA) for 1 min.

EB exposure experiments were performed on a Vistec EBPG 5000plus ES lithography system. EUV patterning properties were examined using the XIL II Beamline of the Swiss Light Source (SLS). The LWR of the lithographic pattern was analyzed by commercial ProSEM software.

RESULTS AND DISCUSSION

The procedure for the synthesis of BPA-6-epoxy is shown in Scheme 1. Epoxy groups are modified around the core of the bisphenol A derivative and can cross-link under acidic conditions after exposure to drive a solubility switch without outgassing.[26] At the same time, the glass transition temperature of the material will increase, reducing the influence of acid diffusion and helping to improve the resolution. Moreover, such materials tend to have superior mechanical strength after cross-linking, and it is expected to overcome the pattern collapse of a small pitch when combined with organic developer such as 4-methyl-2-pentanone (MIBK) and isopropanol (IPA) with relatively low surface tension.
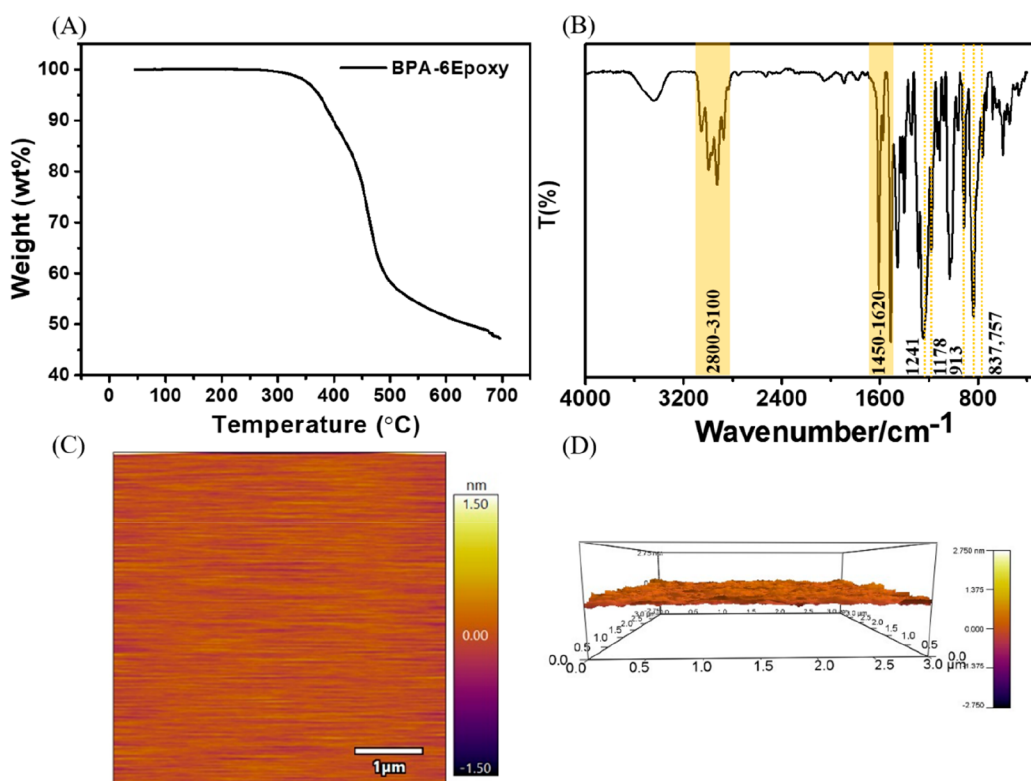
Figure 1. (A) TGA curve of BPA-6-epoxy; (B) IR-FT spectra of BPA-6-epoxy; (C) Surface topography of photoresist film 2 D (C) and 3 D (D) image.

Table 1. EBL Photoresist Formulations Based on Epoxy Negative Photoresist

Formulations	Molecular glass	PAG (wt %)[a]	2-Aminoanthracene (wt %)[b]	Solvent
1	BPA-6-epoxy	10	0	PGMEA
2	BPA-6-epoxy	10	10	PGMEA

[a]Weight percentage with respect to BPA-6-epoxy. [b]Weight percentage with respect to PAG.

Characterization of the BPA-6-Epoxy. *Thermogravimetric Analysis (TGA).* Photoresists are required to have good thermal stability since some thermal treatments are required during the lithography process to remove solvents and accelerate acid diffusion. The thermal behaviors of BPA-6-epoxy were investigated by thermogravimetric analysis, and the results are shown in Figure 1A. The TGA curve shows that the compound only has one-stage decomposition around 350 °C and exhibits good thermal stability with a decomposition amount of less than 5% before 300 °C. The measurement confirms the BPA-6-epoxy can satisfy the bake requirements during the lithography process.

FT-IR. The infrared spectrum of BPA-6-epoxy is shown in Figure 1B. The broad absorption peak at 2900 cm^{-1} was assigned to the C−H stretching vibration. The asymmetric and symmetric stretching vibrations of the C−O−C group were observed at 1241 and 1168 cm^{-1}, respectively. The characteristic absorption at 913 cm^{-1} corresponded to the C−O (epoxy ring) symmetric stretching vibration.[27] In addition, absorption peaks at 837 and 757 cm^{-1} were attributed to −CH$_3$ deformation vibrations, and the peak at 1452 cm^{-1} was assigned to −CH$_2$ deformation vibrations. The absorption peaks from 1450 to 1620 cm^{-1} were assigned to aromatic ring structure. A broad peak appeared at about 3300 cm^{-1}, indicating that the epoxy group is easy to protonate; the sample has been fully dried before IR testing. These characteristic absorption spectra confirmed the presence of the epoxy ring in BPA-6-epoxy.

Film Properties. The optical ellipsometer was used to measure the film thickness, two-dimensional plane, and three-dimensional film surface height fluctuation diagrams show that the surface of BPA-6-epoxy is smooth and free of obvious defects and particles. The surface roughness of BPA-6-epoxy film was analyzed by commercial software, and the surface roughness of BPA-6-epoxy film was measured in the range of 5 × 5 μm^2. The root-mean-square (RMS) value was only 0.29 nm, indicating that the film properties exhibit outstanding film formation behavior that is suitable for high-resolution lithography.

Lithography Performance of BPA-6-Epoxy in EBL. The lithography performance of BPA-6-epoxy was investigated as a negative photoresist by EBL (film thickness: 60 nm). The formulations of BPA-6-epoxy are displayed on Table 1. Figure 2 shows SEM images of half-pitch (HP) 50, 40, and 30 nm of BPA-6-epoxy with and without the addition of 2-aminoanthracene. It is found that BPA-6-epoxy can resolve different HPs from 50 to 30 nm with LWR of 6.1 6.6, and 6.0 nm, respectively, but the HP 30 nm lines appear slightly bridging. When 2-aminoanthracene was introduced into the system (Formulation 2), the pattern quality was improved with lower LWR. In the case of HP 30 nm, bridging was significantly reduced, but exhibits the issue of pattern collapse.
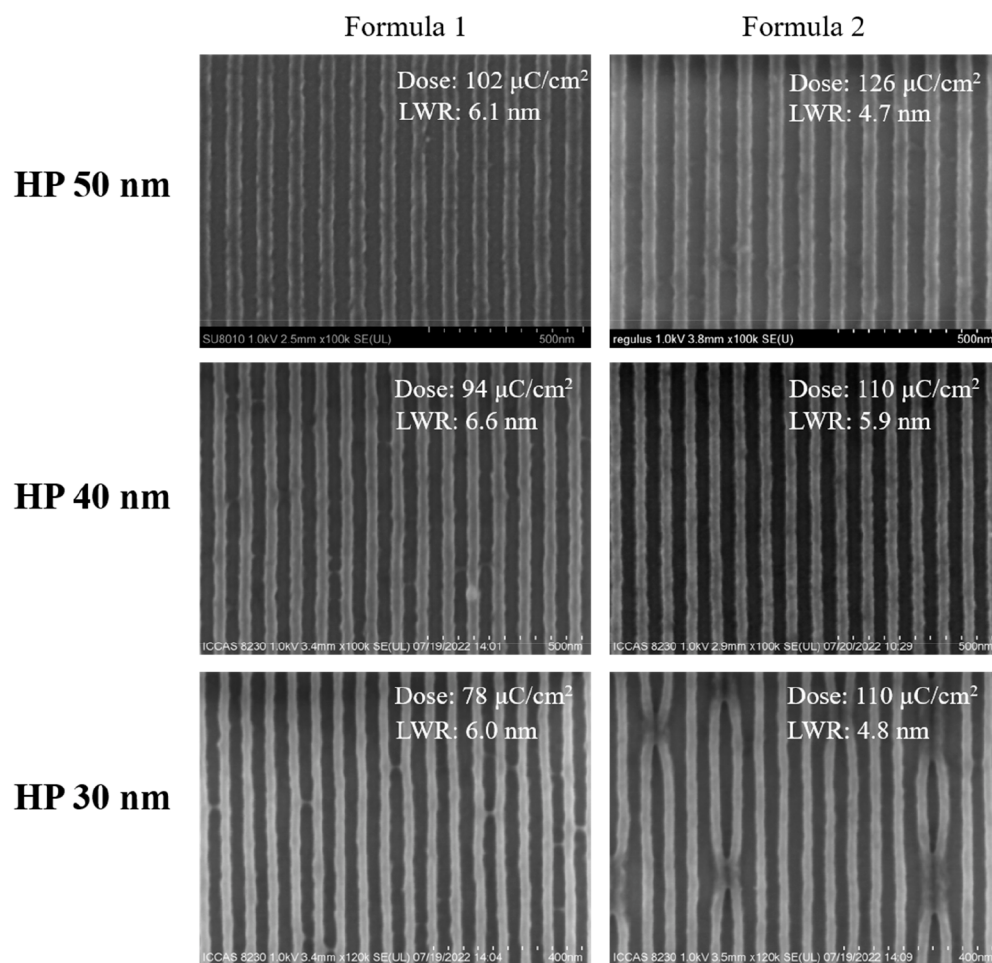
Figure 2. SEM images of lines with HP of 50, 40, and 30 nm for BPA-6-epoxy with and without 2-aminoanthracene (film thickness: 60 nm)
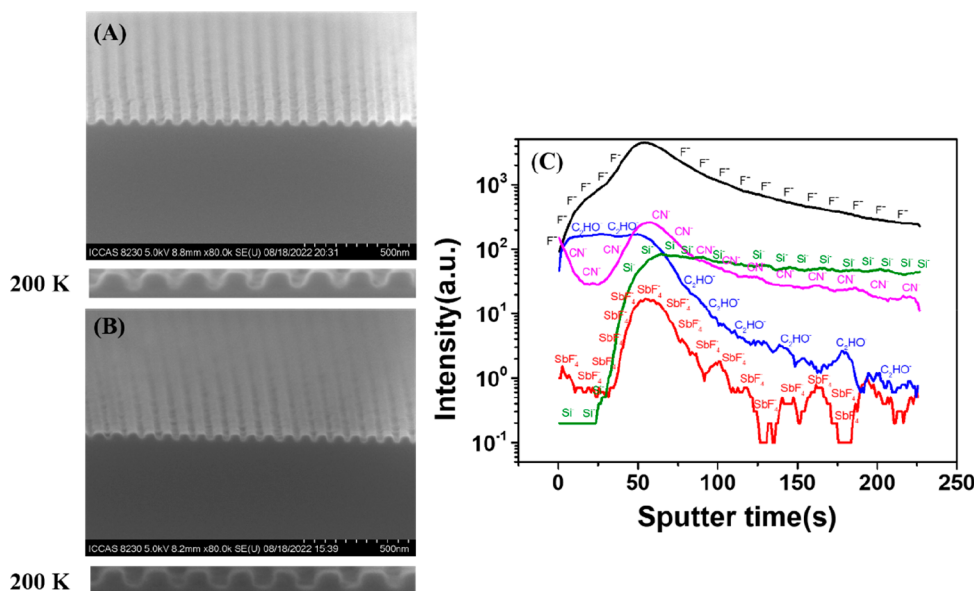

Figure 3. Cross-sectional views of dense lines with HP 50 nm patterns of BPA-6-epoxy with (A) and without 2-aminoanthracene (B), the bottom is a high-magnification SEM image (200 K); (C) TOF-SIMS depth profiles of a series of secondary ion fragments of interest collected at the surface of Formulation 2.

Figure 3 compares the effect of 2-aminoanthracene additive on the HP 50 nm cross section of lines. It can be observed that 2-aminoanthracene additive can improve the edge of the pattern. The Formulation 1 has a trapezoidal shape with narrow top and wide bottom, as shown in Figure 3A. After adding 2-aminoanthracene (Figure 3B), the angle between the

lines and the trenches is close to 90°, and the outline of the pattern is rectangular, which is more regular.

Secondary ion mass spectrometry (SIMS) is a successful technique for analyzing sample surface and has made much progress in photoresist research.[28−30] Bi^{3+} ion was used as a primary ion source to bombard the sample surface, and obtained the distribution information on PAGs, BPA-6-epoxy and 2-aminoanthracene in the vertical direction (Figure 3C). $CN^−$ ion is the characteristic ion of the 2-aminoanthracene and the content change reflects the vertical distribution of 2-aminoanthracene in the film. It can be seen that the 2-aminoanthracene additive is more likely to be distributed at the top and bottom of the film. The difference in the distribution of 2-aminoanthracene at verticals leads to competitive chemical reaction with the onium ion, resulting in different cross-linking densities of the epoxy groups, and thus the lines become steeper and straighter. The nucleophilicity of the nitrogen atom in the molecule and the presence of active hydrogen play a role in regulating the cross-linking reaction of the epoxy group, which may be the reason for the more regular shape of the photoresist pattern at the top and bottom.

For epoxide photoresist systems, strong nucleophiles such as triphenylphosphine (TPP) and triphenylsulfonium triflate (TPS-Tf, a kind of photodecomposable nucleophile) can regulate cross-linking reaction by introducing a chain termination reaction that gives results similar to base quenchers in conventional positive tone chemically amplified photoresists, showing improvements in resolution and line edge roughness in epoxide photoresist systems.[15,16]

In this work, BPA-6-epoxy film was exposed over a large area using a scanning electron microscope (Regulus 8230) with an electron energy of 30 kV and a current of 30 μA to analyze the chemical reaction of 2-aminoanthracene with epoxy ring. The unexposed and exposed wafers were characterized by X-ray photoelectron spectroscopy (XPS). The high-resolution XPS spectra of C 1s, N 1s and O 1s were shown in Figure 4. According to spectra of C 1s (Figure 4A), the most intensive peak at 284.8 eV was assigned to the C−C and C−H bonds in the film. The peak at 286.7 eV corresponded to C−O−C structure in epoxy ring. After exposure, a new signal was observed at 288.8 eV, which was in accordance with the peak of −N−C=O.[31]

In addition, a new peak at 401.6 eV was attributed to the formation of N−C bond after e-beam exposure as shown in Figure 4C. As for spectra of O 1s (Figure 4B), the peak shifts from 533.4 to 532.5 eV after exposure, which might be caused by the chemical reaction of 2-aminoanthracene with epoxide ring. The XPS spectra of BPA-6-epoxy without 2-aminoantheacene after exposure are shown in Figure S3. It indicates that 2-aminoanthracene is indeed involved in the cross-linking reaction of epoxide ring, thus improving the cross section of exposure pattern for EBL.

Lithography Performance of BPA-6-Epoxy in EUVL. Applying BPA-6-epoxy with additive 2-aminoanthracene to extreme ultraviolet lithography (EUV) can also get better lithography results. Photoresist formulations in Table 2 were spin-coated on a silicon wafer for EUV lithography. Figure 5 compares the impact of the 2-aminoanthracene additive on different HP lithography patterns. When the formulation (PR-1) does not contain 2-aminoanthracene, lines with critical dimension (CD) of 25 and 22 nm 1:1 L/S can be obtained and the LWR is 4.9 and 6.9 nm, respectively. The introduction of 2-aminoanthracene can effectively improve the roughness of
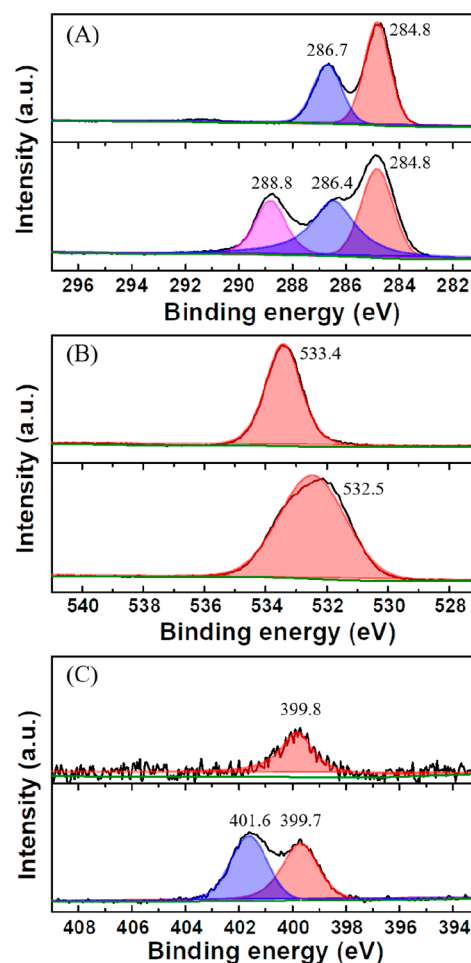
Figure 4. High-resolution XPS spectra of (A) C 1s, (B) O 1s and (C) N 1s of BPA-6-epoxy with 2-aminoanthracene before (top) and after e-beam exposure (bottom).

the pattern. When the additive content is 10% with respect to PAG (PR-2), the LWR of the corresponding pattern is 3.8 and 3.0 nm, respectively (a decrease of 22.4% and 56.5%). The imaging dose increases from 15.4 to 17.5 mJ/cm^2 for HP 22 nm on the premise of sacrificing sensitivity simultaneously, which is acceptable. It is demonstrated that 2-aminoanthracene additive can reduce LWR by regulating epoxy cross-linking reaction in EUVL which is similar to the quencher base in the positive-tone photoresist system.

In order to comprehensively understand the effect of photoresist formulation on LWR, power density spectrum (PSD) was used to analyze the roughness and gave more detailed information on photolithography patterns, which can provide theoretical guidance for the design of new photoresists.[32−35] PSD regards roughness as noise and studies the spatial variation period of roughness with the length of the line or trench. PSD function describes the random process of line edge profile waveform from the perspective of frequency domain, decomposes the surface profile into different Fourier components, and can reflect most of the information on line edge spatial frequency characteristics. It is advantageous to analyze the reasons for the formation of roughness so as to reduce the roughness of the pattern. Figure 6 shows the spectrum analysis of roughness calculation under different formulation. It is confirmed through amplitude analysis that the addition of 2-aminoanthracene can significantly reduce the

Table 2. EUV Photoresist Formulations Based on Epoxy Negative Photoresists

Formulations	Molecular glass	PAG (wt %)[a]	2-Aminoanthracene (wt %)[b]	Solvent
PR-1	BPA-6-epoxy	10	0	PGMEA
PR-2	BPA-6-epoxy	10	10	PGMEA
PR-3	BPA-6-epoxy	10	20	PGMEA
PR-4	BPA-6-epoxy	10	30	PGMEA
PR-5	BPA-6-epoxy	7.5	10	PGMEA

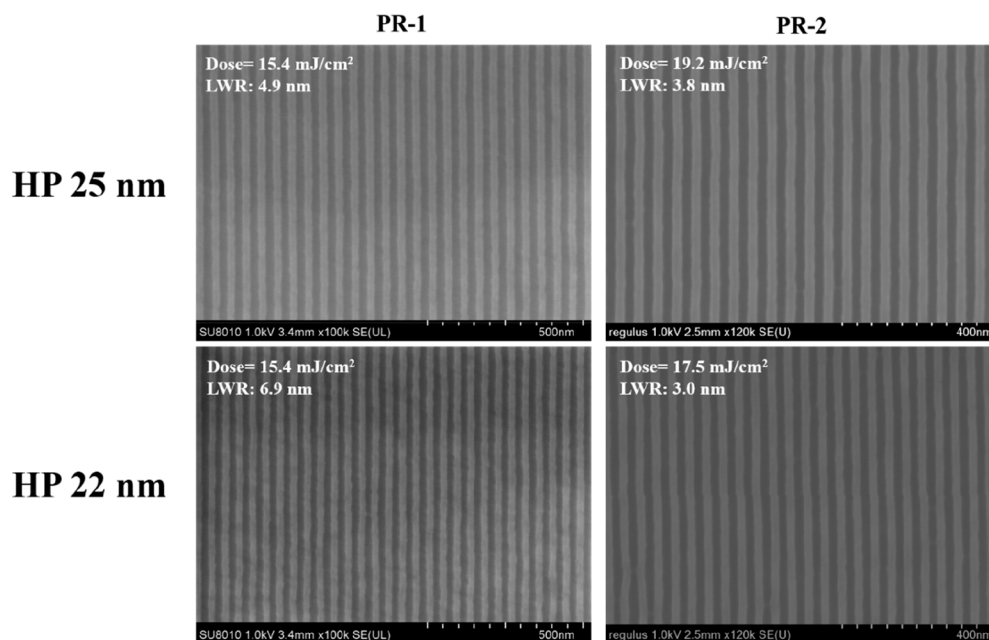[a]Weight percentage with respect to BPA-6-epoxy. [b]Weight percentage with respect to PAG.

Figure 5. High-resolution SEM images of BPA-6-epoxy with and without 10% 2-aminoanthracene for HP 25 and 22 nm. The critical dimensions are 25 and 22 nm with 1:1 L/S, respectively (film thickness: 34 nm).
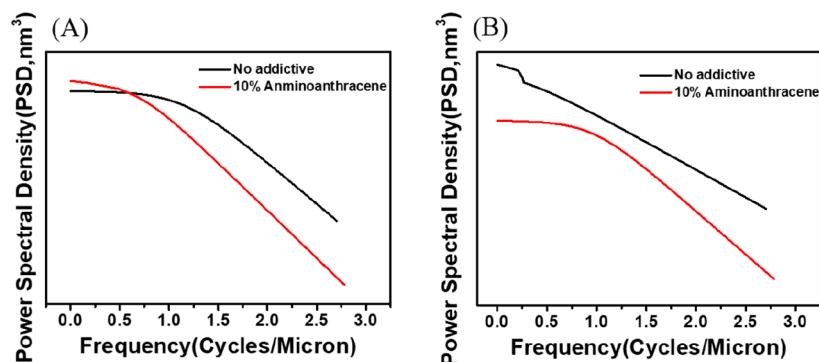

Figure 6. PSD curves of BPA-6-epoxy with and without 10% 2-aminoanthracene for (A) HP 25 nm and (B) HP 22 nm after EUVL.

roughness of HP 25 nm and HP 22 nm; the PSD curve indicated that HP 25 nm lines mainly improve the roughness in medium and high frequencies, and HP 22 nm patterns' roughness optimization occurs in the whole range of medium, low, and high frequencies.

Moreover, the lithography performances of PR-2 and PR-5 were compared to further study the role of 2-aminoanthracene additive in the epoxy system. The overall concentration of PR-5 PAG and 2-aminoanthracene decreased, from 10% PAG and 10% 2-aminoanthracene for PR-2 to 7.5% PAG and 10% 2-aminoanthracene for PR-5, but the sensitivity was improved, from 19.2 mJ/cm^2 to 14.9 mJ/cm^2 for HP 25 nm and from 17.5 mJ/cm^2 to 13.8 mJ/cm^2 for HP 22 nm, as shown in

Figure 7. It is supposed that 2-aminoanthracene was an amine and has a nucleophilic property, which can terminate the epoxy cross-linking reaction, so the sensitivity is decreased; on the other hand, it acts as an antenna, which is equal to a sensitizer and can improve the sensitivity.

Figure 8 shows results of EUVL of the BPA-6-epoxy system at three different contents with the gradual increase of 2-aminoanthracene content (10% to 30%). By comparing the lithography pattern of each HP, it can be concluded that the contrast of the result decreases with the increase of the content of 2-aminoanthracene. In the case of HP 22 nm patterns, significant line breaks are observed, and the quality decreases dramatically. As a result, it can be seen that the EUV
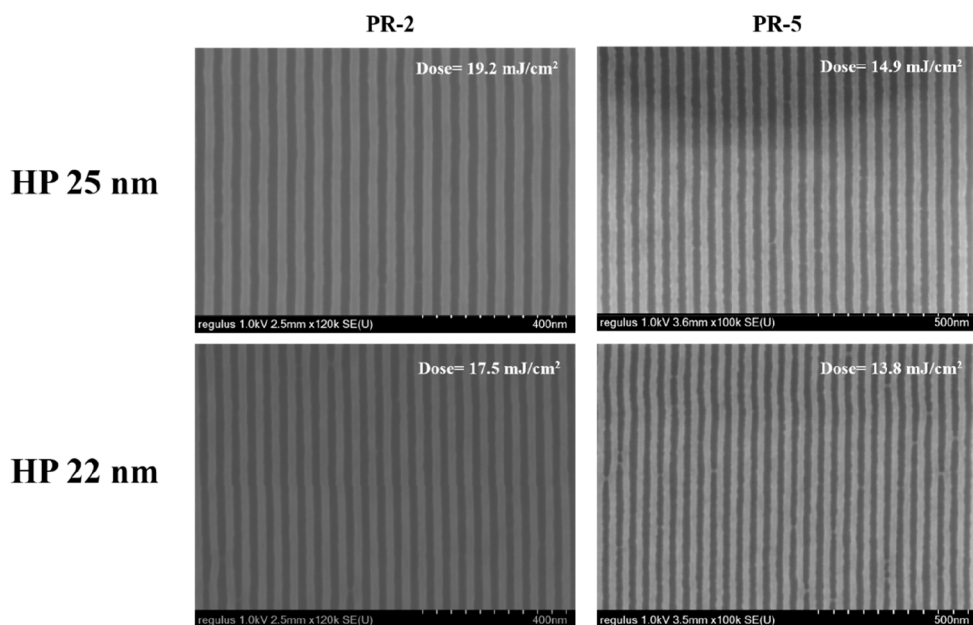
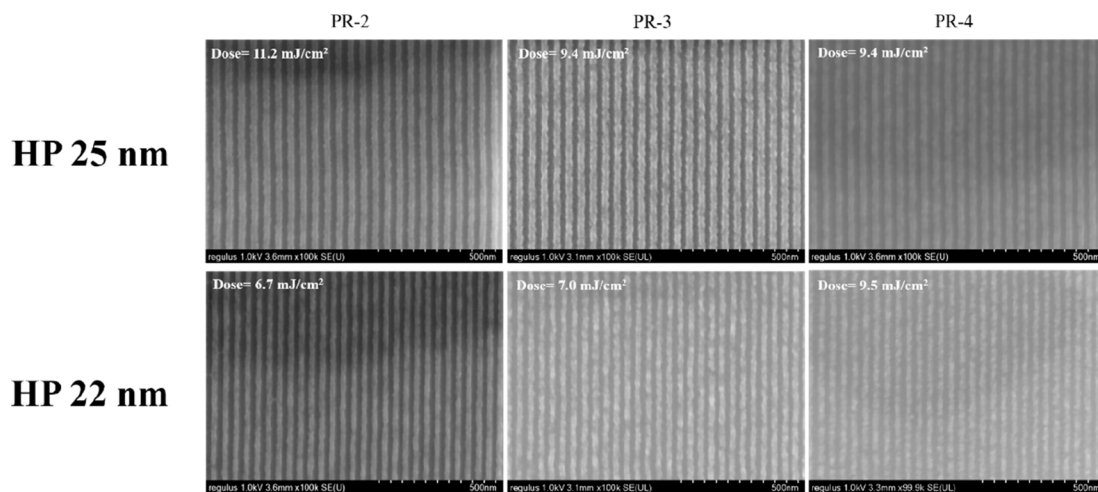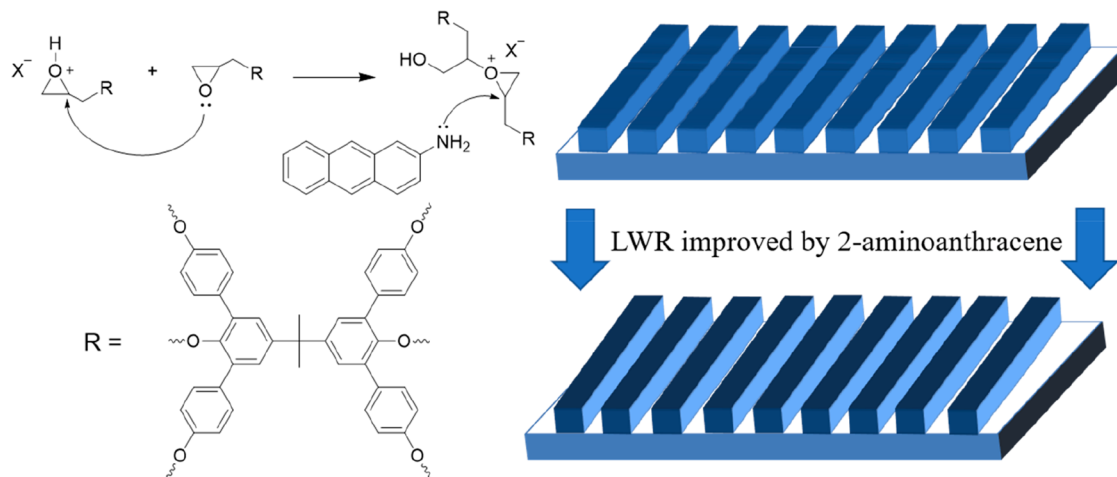**Figure 7.** SEM images of PR-2 and PR-5 for HP 25 and 22 nm.

Figure 8. SEM images of BPA-6-epoxy with different formulations (PR-2, PR-3, PR-4) for HP 25 and 22 nm.

Scheme 2. Proposed Mechanism for the Role of 2-Aminoanthracene in Lithographic Process

lithography pattern was better when 2-aminoanthracene content was 10% compared to the other experiment groups.

Lithographic Mechanism of 2-Aminoanthracene in BPA-6-Epoxy. Based on literature and experimental results, the role of 2-aminoanthracene in BPA-6-epoxy can be proposed in Scheme 2. It is confirmed that 2-aminoanthracene is involved in regulating the cross-linking reactions of epoxy groups as a nucleophilic reagent; the nucleophilic nitrogen in 2-aminoanthracene attacked the epoxy groups after exposure, effecting the reaction rate and the distance of ring-opening polymerization in the original system. Meanwhile, it also reduced the diffusion of active species by introducing a chain termination reaction, which gives results similar to those of base quenchers in conventional positive-tone chemically amplified photoresists, showing improvements in LWR in epoxide photoresist systems.

CONCLUSIONS

In this work, a bisphenol A derivative, BPA-6-epoxy, was designed and synthesized, which can serve as negative-tone photoresist for EBL and EUVL. When 2-aminoanthracene was introduced as a nucleophilic additive in EBL, the LWR of different HPs (HP 50, 40, and 30 nm) was improved. It is demonstrated that additives can improve the outline of the stripes more clearly in EBL. Secondary ion mass spectrometry (SIMS) analysis indicates that 2-aminoanthracene is abundant in the silicon substrate, which achieves the goal of regulating the epoxy cross-linking reaction and optimizes the pattern outline. The high-resolution XPS spectra of C 1s, O 1s, and N 1s affirm that 2-aminoanthracene is indeed involved in the cross-linking reaction of the epoxy ring, thus improving the cross section of the exposure pattern in EBL. Besides, 2-aminoanthracene can reduce the LWR of HP 25 and HP 22 nm patterns by 1.1 nm (from 4.9 to 3.8 nm, 22.4% decrease) and 3.9 nm (from 6.9 to 3.0 nm, 56.5% decrease) in EUVL obviously. Combined with the energy density spectrum (PSD), it is found that 2-aminoanthracene can reduce the medium and high frequency roughness in the HP 25 nm and the roughness of the whole frequency range in the HP 22 nm, respectively. In addition, it is found that when the additive 2-aminoanthracene accounts for 10% (weight percentage with respect to PAG), the lithography performance in EUVL is the best. It reveals that high-resolution molecular glass photoresist can be regulated by 2-aminoanthracene, giving useful guidance for improving the lithography performance.

ASSOCIATED CONTENT

Supporting Information

The Supporting Information is available free of charge at https://pubs.acs.org/doi/10.1021/acsomega.2c07711.

^{1}H NMR and ^{13}C NMR spectra of BPA-6-epoxy; XPS spectra of BPA-6-epoxy film without 2-aminoantheacene after exposure (PDF)

AUTHOR INFORMATION

Corresponding Authors

Xudong Guo − *Beijing National Laboratory for Molecular Sciences, Key Laboratory of Photochemistry, Institute of Chemistry, University of Chinese Academy of Sciences, Chinese Academy of Sciences, Beijing 100190, China;* orcid.org/0000-0002-2012-4399; Email: scoopguo@iccas.ac.cn

Shuangqing Wang − *Beijing National Laboratory for Molecular Sciences, Key Laboratory of Photochemistry, Institute of Chemistry, University of Chinese Academy of Sciences, Chinese Academy of Sciences, Beijing 100190, China;* orcid.org/0000-0002-8281-9399; Email: g1704@iccas.ac.cn

Guoqiang Yang − *Beijing National Laboratory for Molecular Sciences, Key Laboratory of Photochemistry, Institute of Chemistry, University of Chinese Academy of Sciences, Chinese Academy of Sciences, Beijing 100190, China;* orcid.org/0000-0003-0726-2217; Email: gqyang@iccas.ac.cn

Authors

Siliang Zhang − *Beijing National Laboratory for Molecular Sciences, Key Laboratory of Photochemistry, Institute of Chemistry, University of Chinese Academy of Sciences, Chinese Academy of Sciences, Beijing 100190, China*

Long Chen − *Beijing National Laboratory for Molecular Sciences, Key Laboratory of Photochemistry, Institute of Chemistry, University of Chinese Academy of Sciences, Chinese Academy of Sciences, Beijing 100190, China*

Jiaxing Gao − *Beijing National Laboratory for Molecular Sciences, Key Laboratory of Photochemistry, Institute of Chemistry, University of Chinese Academy of Sciences, Chinese Academy of Sciences, Beijing 100190, China*

Xuewen Cui − *Beijing National Laboratory for Molecular Sciences, Key Laboratory of Photochemistry, Institute of Chemistry, University of Chinese Academy of Sciences, Chinese Academy of Sciences, Beijing 100190, China*

Xue Cong − *Beijing National Laboratory for Molecular Sciences, Key Laboratory of Photochemistry, Institute of Chemistry, University of Chinese Academy of Sciences, Chinese Academy of Sciences, Beijing 100190, China*

Rui Hu − *Beijing National Laboratory for Molecular Sciences, Key Laboratory of Photochemistry, Institute of Chemistry, University of Chinese Academy of Sciences, Chinese Academy of Sciences, Beijing 100190, China;* orcid.org/0000-0003-4949-6214

Jinping Chen − *Key Laboratory of Photochemical Conversion and Optoelectronic Materials, Technical Institute of Physics and Chemistry, University of Chinese Academy of Sciences, Chinese Academy of Sciences, Beijing 100190, China;* orcid.org/0000-0002-5632-2290

Yi Li − *Key Laboratory of Photochemical Conversion and Optoelectronic Materials, Technical Institute of Physics and Chemistry, University of Chinese Academy of Sciences, Chinese Academy of Sciences, Beijing 100190, China;* orcid.org/0000-0002-7018-180X

Complete contact information is available at: https://pubs.acs.org/10.1021/acsomega.2c07711

Author Contributions

§S.Z. and L.C. contributed equally to this work.

Notes

The authors declare no competing financial interest.

ACKNOWLEDGMENTS

National Center for Nanoscience and Technology of China for EBL experiments and the XIL II Beamline of the Swiss Light Source for EUV experiments.

■ REFERENCES

(1) Miyazaki, J.; Yen, A. EUV Lithography Technology for High-volume Production of Semiconductor Devices. *J. Photopolym. Sci. Technol.* **2019**, *32*, 195−201.

(2) Luo, S.; Hoff, B. H.; Maier, S. A.; de Mello, J. C. Scalable Fabrication of Metallic Nanogaps at the Sub-10 nm Level. *Adv. Sci. (Weinh)* **2021**, *8*, No. 2102756.

(3) Luo, C.; Xu, C.; Lv, L.; Li, H.; Huang, X.; Liu, W. Review of Recent Advances in Inorganic Photoresists. *RSC Adv.* **2020**, *10*, 8385−8395.

(4) Ito, H.; Willson, C. G. Chemical Amplification in The Desigy of Dry Developing Resist Materials. *Polym. Eng. Sci.* **1983**, *23*, 1012−1018.

(5) Moinuddin, M. G.; Kumar, R.; Yogesh, M.; Sharma, S.; Sahani, M.; Sharma, S. K.; Gonsalves, K. E. Functionalized Ag Nanoparticles Embedded in Polymer Resists for High-Resolution Lithography. *ACS Appl. Nano Mater.* **2020**, *3*, 8651−8661.

(6) Oleksak, R. P.; Ruther, R. E.; Luo, F.; Amador, J. M.; Decker, S. R.; Jackson, M. N.; Motley, J. R.; Stowers, J. K.; Johnson, D. W.; Garfunkel, E. L.; Keszler, D. A.; Herman, G. S. Evaluation of Thermal and Radiation Induced Chemistries of Metal Oxo−Hydroxo Clusters for Next-Generation Nanoscale Inorganic Resists. *ACS Appl. Nano Mater.* **2018**, *1*, 4548−4556.

(7) Wang, Y. K.; Chen, J. P.; Zeng, Y.; Yu, T. J.; Guo, X. D.; Wang, S. Q.; Allenet, T.; Vockenhuber, M.; Ekinci, Y.; Zhao, J.; Yang, S. M.; Wu, Y. Y.; Yang, G. Q.; Li, Y. Molecular Glass Resists Based on Tetraphenylsilane Derivatives: Effect of Protecting Ratios on Advanced Lithography. *ACS Omega* **2022**, *7*, 29266−29273.

(8) Deng, J. Y.; Bailey, S.; Jiang, S. Y.; Ober, C. K. Modular Synthesis of Phthalaldehyde Derivatives Enabling Access to Photoacid Generator-Bound Self-Immolative Polymer Resists with Next-Generation Photolithographic Properties. *J. Am. Chem. Soc.* **2022**, *144*, 19508−19529.

(9) Sysova, O.; Durin, P.; Gablin, C.; Leonard, D.; Teolis, A.; Trombotto, S.; Delair, T.; Berling, D.; Servin, I.; Tiron, R.; Bazin, A.; Leclercq, J. L.; Chevolot, Y.; Soppera, O. Chitosan as a Water-Developable 193 nm Photoresist for Green Photolithography. *ACS Appl. Polym. Mater.* **2022**, *4*, 4508−4519.

(10) Yogesh, M.; Moinuddin, M. G.; Chauhan, M.; Sharma, S. K.; Ghosh, S.; Gonsalves, K. E. Organoiodine Functionality Bearing Resists for Electron-Beam and Helium Ion Beam Lithography: Complex and Sub-16 nm Patterning. *ACS Appl. Electron. Mater.* **2021**, *3*, 1996−2004.

(11) Lawson, R. A.; Lee, C.-T.; Henderson, C. L.; Whetsell, R.; Tolbert, L.; Yueh, W. Influence of Solubility Switching Mechanism on Resist Performance in Molecular Glass Resists. *J. Vac. Sci. Technol. B* **2007**, *25*, 2140.

(12) Lawson, R. A.; Lee, C.-T.; Yueh, W.; Tolbert, L.; Henderson, C. L. Epoxide Functionalized Molecular Resists for High Resolution Electron-beam Lithography. *Microelectron. Eng.* **2008**, *85*, 959−962.

(13) Lawson, R. A.; Lee, C.-T.; Tolbert, L. M.; Younkin, T. R.; Henderson, C. L. High Resolution Negative Tone Molecular Resist Based on Di-functional Epoxide Polymerization. *Microelectron. Eng.* **2009**, *86*, 734−737.

(14) Lawson, R. A.; Noga, D. E.; Younkin, T. R.; Tolbert, L. M.; Henderson, C. L. Negative Tone Molecular Resists Using Cationic Polymerization: Comparison of Epoxide and Oxetane Functional Groups. *J. Vac. Sci. Technol. B* **2009**, *27*, 2998.

(15) Wallow, T. I.; Hohle, C. K.; Lawson, R. A.; Chun, J. S.; Neisser, M.; Tolbert, L. M.; Henderson, C. L. Positive Tone Cross-linked Resists Based on Photoacid Inhibition of cross linking. *Proc. SPIE* **2014**, *0951*, No. 90510E.

(16) Wallow, T. I.; Hohle, C. K.; Lawson, R. A.; Chun, J. S.; Neisser, M.; Tolbert, L. M.; Henderson, C. L. Methods of Controlling Cross-linking in Negative-tone Resists. *Proc. SPIE* **2014**, *9051*, No. 90510Q.

(17) Manouras, T.; Kazazis, D.; Ekinci, Y.; Felix, N. M.; Lio, A. Chemically-amplified Backbone Scission (CABS) Resist for EUV Lithography. *Proc. SPIE* **2021**, *11609*, No. 116090H.

(18) Macdonald, S. A.; Clecak, N. J.; Wendt, H. R.; Willson, C. G.; Snyder, C. D.; Knors, C. J.; Deyoe, N. B.; Maltabes, J. G.; Morrow, J. R.; McGuire, A. E.; Holmes, S. J. Airborne Chemical Contamination of a Chemically Amplified Resist. *Proc. SPIE* **1991**, *1466*, 2−12.

(19) Ito, H. Chemical Amplification Resists: History and Development Within IBM. *IBM J. Res. Dev.* **1997**, *41*, 119−130.

(20) Ito, H. Rise of Chemical Amplification Resists From Laboratory Curiosity to Paradigm Enabling Moore's Law. *Proc. SPIE* **2008**, *6923*, No. 692302.

(21) Patsis, G. P.; Gogolides, E.; Van Werden, K. Effects of Photoresist Polymer Molecular Weight and Acid-diffusion on Line-edge Roughness. *Jpn. J. Appl. Phys.* **2005**, *44*, 6341−6348.

(22) Cutler, C.; Thackeray, J. W.; Trefonas, P.; Millward, D.; Lee, C.-B.; Mack, C. Pattern Roughness Analysis Using Power Spectral Density: Application and Impact in Photoresist Formulation. *J. Micro/ Nanopattern. Mater., Metrol.* **2021**, *20*, No. 010901.

(23) Sturtevant, J. L.; Van Steenwinckel, D.; Lammers, J. H.; Leunissen, L. H. A.; Kwinten, J. A. J. M. Lithographic Importance of Acid Diffusion in Chemically Amplified Resists. *Proc. SPIE* **2005**, *5753*, 269−280.

(24) Yang, G. Q.; Wang, Y. F.; Chen, L.; Yu, J. T.; Hu, R.; Guo, X. D; Wang, S. Q. Bisphenol A Derivative, Preparation Method Therefor, and Application Thereof in Photolithography. U.S. Patent Application No. 17/753898, 2022.

(25) Peng, X. M.; Wang, Y. F.; Xu, J.; Yuan, H.; Wang, L. Q.; Zhang, T.; Guo, X. D.; Wang, S. Q.; Li, Y.; Yang, G. Q. Molecular Glass Photoresists with High Resolution, Low LER, and High Sensitivity for EUV Lithography. *Macromol. Mater. Eng.* **2018**, *303*, No. 1700654.

(26) Chen, L.; Xu, J.; Yuan, H.; Yang, S.; Wang, L.; Wu, Y.; Zhao, J.; Chen, M.; Liu, H.; Li, S.; Tai, R.; Wang, S.; Yang, G. Outgassing Analysis of Molecular Glass Photoresists Under EUV Irradiation. *Sci. China Chem.* **2014**, *57*, 1746−1750.

(27) Ding, Y.; Xin, Y.; Zhang, Q.; Zou, Y. Acrylic Resins with Oxetane Pendant Groups for Free Radical and Cationic Dual-curing Photoresists. *Mater. Des.* **2022**, *213*, No. 110370.

(28) Gajos, K.; Budkowski, A.; Petrou, P.; Awsiuk, K.; Misiakos, K.; Raptis, I.; Kakabakos, S. Spatially Selective Biomolecules Immobilization on Silicon Nitride Waveguides Through Contact Printing onto Plasma Treated Photolithographic Micropattern: Step-by-step Analysis with TOF-SIMS Chemical imaging. *Appl. Surf. Sci.* **2020**, *506*, No. 145002.

(29) Man, N.; Okumura, H.; Oizumi, H.; Nagai, N.; Seki, H.; Nishiyama, I. Depth Profile Analysis of Chemically Amplified Resist by Using TOF-SIMS with Gradient Shaving Preparations. *Appl. Surf. Sci.* **2004**, *231*, 353−356.

(30) Spampinato, V.; Franquet, A.; De Simone, D.; Pollentier, I.; Pirkl, A.; Oka, H.; van der Heide, P. SIMS Analysis of Thin EUV Photoresist Films. *Anal. Chem.* **2022**, *94*, 2408−2415.

(31) Sysova, O.; Durin, P.; Gablin, C.; Léonard, D.; Téolis, A.; Trombotto, S.; Delair, T.; Berling, D.; Servin, I.; Tiron, R.; Bazin, A.; Leclercq, J.-L.; Chevolot, Y.; Soppera, O. Chitosan as a Water-Developable 193 nm Photoresist for Green Photolithography. *ACS Appl. Polym. Mater.* **2022**, *4*, 4508−4519.

(32) Liu, E.; Hegazy, A.; Choi, H.; Weires, M.; Brainard, R.; Denbeaux, G. Characterization of Surface Variation of Chemically Amplified Photoresist to Evaluate Extreme Ultraviolet Lithography Stochastics Effects. *J. Photopolym. Sci. Technol.* **2021**, *34*, 63−70.

(33) Mack, C. A. Reaction-diffusion power spectral density. *J.Micro/ Nanolithogr., MEMS, MOEMS* **2012**, *11*, No. 043007.

(34) Hiraiwa, A.; Nishida, A. Power Spectrum of Smoothed Line-Edge and Line-Width Roughness. *Jpn. J. Appl. Phys.* **2011**, *50*, No. 086502.

(35) Liu, E.; Hegazy, A.; Choi, H.; Weires, M.; Brainard, R.; Denbeaux, G. Characterization of Surface Variation of Chemically Amplified Photoresist to Evaluate Extreme Ultraviolet Lithography Stochastics Effects. *J. Photopolym. Sci. Technol.* **2021**, *34*, 63−70.